Analyzing Lanthanide-Induced Shifts in the NMR Spectra of Lanthanide(III) Complexes Derived from 1,4,7,10-Tetrakis(*N,N*-diethylacetamido)-1,4,7,10-tetraazacyclododecane

John H. Forsberg,* Robert M. Delaney, Qian Zhao, George Harakas, and Rubin Chandran

Departments of Chemistry and Physics, Saint Louis University, St. Louis, Missouri 63103

Received September 30, 1994[⊗]

Variable-temperature ^1H and ^{13}C NMR spectra have been obtained for solutions of lanthanide(III) complexes derived from 1,4,7,10-tetrakis(*N,N*-diethylacetamido)-1,4,7,10-tetraazacyclododecane in deuterated acetonitrile. The lanthanide-induced shifts (LIS) observed in the spectra of the paramagnetic complexes (Ln = Pr, Nd, Sm, Eu, Tb, Dy, Ho, Er, Tm, and Yb) are analyzed using a linear least-squares procedure involving the five components of the traceless part of the magnetic susceptibility tensor as fitting parameters (^{13}C data is limited to Ln = Pr, Nd, Sm, and Eu). No assumptions are made regarding the orientation of the molecular coordinate system and principal magnetic axis system in this method of analysis. Furthermore, by using a linear least-squares fitting of the data, we establish that it is possible to allow a computer program to permute LIS values over any number of nuclei and determine which particular assignment gives the best fit of the LIS data. A new method of evaluating the contact component of the LIS in the proton spectra is introduced. Molecular mechanics calculations are combined with analyses of LIS data to determine structures of the complexes in solution. Through such an approach, we establish that the eight-coordinate lanthanide ions are encapsulated by the octadentate macrocyclic ligand, with the four nitrogen atoms and four oxygen atoms situated at the vertices of a distorted square antiprism having C_4 symmetry (the rotational angle between the two square pyramids is 47°). The lanthanide ions lie above the plane of nitrogen atoms of the macrocycle, with the distance decreasing from 1.74 to 1.41 Å across the lanthanide series. The distance to the mean plane of donor oxygen atoms increases from 0.63 to 0.83 Å across the series. The $Ln^{3+}-N$ and $Ln^{3+}-O$ bond distances range from 2.82 to 2.54 Å and 2.47 to 2.21 Å, respectively. The NMR data establish that each complex exists in solution as a single pair of enantiomers. Analysis of the LIS data establishes that the isomer with each ethylenediamine ring of the macrocycle in the λ conformation with clockwise rotation of the pendant arms, or its enantiomer, is favored in solution.

Introduction

The value of paramagnetic lanthanide ions as NMR probes to determine the structure of molecules in solution is well documented.[1] The binding of a ligand to a paramagnetic lanthanide ion induces frequency shifts in the NMR spectrum (LIS) of the ligand relative to that observed for the corresponding diamagnetic complex. The LIS has two contributions, the Fermi contact (δ_c) and the dipolar or pseudocontact shifts (δ_{pc}):

$$LIS = \delta_c + \delta_{pc} \tag{1}$$

The contact shift is given by

$$\delta_c = \frac{2\pi\beta}{3kT\gamma}\frac{A}{h}\langle S_z \rangle \tag{2}$$

where β is the Bohr magneton, k is the Boltzmann constant, γ is the gyromagnetic ratio, A/h is the hyperfine coupling constant in frequency units, and $\langle S_z \rangle$ is the electron-spin expectation value, which has been tabulated for each Ln^{3+} ion.[2,3]

Structural information is obtained from the pseudocontact shift, which is given by[4]

$$\delta_{pc}^i = \frac{1}{2N}\Bigg[\left(\chi_{zz} - \frac{1}{3}Tr\chi\right)\left\langle\frac{3\cos^2\theta - 1}{r^3}\right\rangle + (\chi_{xx} - \chi_{yy})\left\langle\frac{\sin^2\theta\cos 2\varphi}{r^3}\right\rangle\Bigg] + \frac{1}{N}\Bigg[\chi_{xy}\left\langle\frac{\sin^2\theta\sin 2\varphi}{r^3}\right\rangle + \chi_{xz}\left\langle\frac{\sin 2\theta\cos\varphi}{r^3}\right\rangle + \chi_{yz}\left\langle\frac{\sin 2\theta\sin\varphi}{r^3}\right\rangle\Bigg] \tag{3}$$

where r, θ, and φ are the spherical coordinates of the *i*th nucleus in the molecular coordinate system with the Ln^{3+} ion located at the origin and χ, the magnetic susceptibility tensor, is taken to be a symmetric tensor and $Tr\chi = \chi_{xx} + \chi_{yy} + \chi_{zz}$. In the principal magnetic axis system, the last three terms of eq 3 vanish (χ is diagonal in the principal axis system), and only the first term remains for the special case of axial symmetry ($\chi_{xx} = \chi_{yy}$). In both eqs 2 and 3, positive shifts are to higher frequency (downfield). Recently, Kemple et al.[4] introduced a new procedure of analyzing LIS data which makes no assumptions regarding the location of the principal magnetic axes or symmetry of the complex. Following the Kemple procedure, geometric factors are calculated in the molecular coordinate system and then a five-parameter [$(\chi_{zz} - \frac{1}{3} Tr\chi)$, $(\chi_{xx} - \chi_{yy})$, χ_{xy}, χ_{xz}, and χ_{yz}] linear least-squares search minimizes the differences between calculated and observed δ_{pc} values according to an agreement factor[5] defined in eq 4. Since δ_{pc} depends only on the anisotropy (traceless part χ') of the

[⊗] Abstract published in *Advance ACS Abstracts*, June 15, 1995.
(1) Sherry, A. D.; Geraldes, C. F. G. C. *Lanthanide Probes in Life, Chemical and Earth Sciences*; Bünzli, J.-C. G., Choppin, G. R., Eds.; Elsevier: Amsterdam, 1989; Chapter 4.
(2) Golding, R. M.; Halton, M. P. *Aust. J. Chem.* **1972**, *25*, 2577.
(3) Pinkerton, A. A.; Rossier, M.; Stavros, S. *J. Magn. Reson.* **1985**, *64*, 420.
(4) Kemple, M. D.; Ray, B. D.; Lipkowitz, K. B.; Prendergast, F. G.; Rao, B. D. N. *J. Am. Chem. Soc.* **1988**, *110*, 8275.

(5) (a) Willcott, M. R.; Lenkinski, R. E.; Davis, R. E. *J. Am. Chem. Soc.* **1972**, *94*, 1742. (b) Davis, R. E.; Willcott, M. R. *J. Am. Chem. Soc.* **1972**, *94*, 1744.

$$R = \left(\frac{\sum_i (\delta_{calc} - \delta_{obs})_i^2}{\sum_i \delta_{obsi}^2} \right)^{1/2} \quad (4)$$

susceptibility tensor χ, the determination of these five fitting parameters is sufficient to determine the principal values of χ'. The principal directions of χ' (and χ) are then determined by diagonalization of χ'.

It is often the case that an unequivocal assignment of all the peaks in a spectrum of a paramagnetic complex is not possible, especially when there are a large number of equally intense, featureless peaks in a spectrum. By using a linear least-squares fitting of the data, we will show that it is possible to allow the program to permute LIS values over any number of selected nuclei, thereby determining which particular assignment of peaks gives the best fit to the LIS data.

To establish the efficacy of our methods to analyze LIS data, we sought a ligand that would form structurally rigid complexes with the Ln^{3+} ions on the NMR time scale. Although Ln^{3+} complexes are among the most labile and exhibit a variety of structures in solution, Desreux et al.[6] discovered that complexes derived from macrocyclic ligands containing acetate groups as pendant arms such as 1,4,7,10-tetraazacyclododecane-*N,N′,N″,N‴*-tetraacetic acid (H4DOTA) are stereochemically rigid on the NMR time scale. The demonstrated ability of [Gd(DOTA)]⁻ as an effective contrast agent in magnetic resonance imaging (MRI) has prompted much interest in kinetic and thermodynamic as well as NMR studies of lanthanide complexes derived from other DOTA analogues.[7-17] Since neutral derivatives of DOTA had not been investigated at the time we initiated our study,[18] we decided to examine the ligating properties of 1,4,7,10-tetrakis(*N,N*-diethylacetamido)-1,4,7,10-tetraazacyclododecane (**1**). We report here our NMR studies of diamagnetic and paramagnetic lanthanide complexes derived from **1**. On the basis of structures reported for lanthanide complexes derived from DOTA and its analogues,[6b,8,9] it is expected that **1** will coordinate Ln^{3+} ions through the four nitrogen atoms of the macrocyclic ring and four oxygen atoms of the pendant arms, resulting in an octadentate complex.
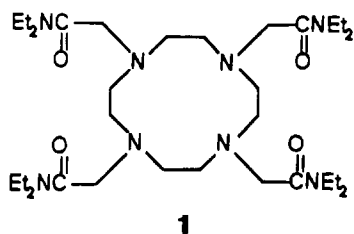
1

Analysis of the pseudocontact shifts is generally initiated by assuming some structure for the complex in solution, thereby allowing calculation of the geometric factors. A common practice is to assume that the structure in solution is the same as that determined in the solid state by X-ray crystallography. However, solid state structures may be poor approximations for structures in solution. An alternative approach is to use molecular mechanics calculations to approximate the structure of a complex.[19] The problem is that Ln^{3+}−donor atom interactions are primarily electrostatic, and as a result, the coordination numbers and geometry of lanthanide complexes are dictated primarily by the steric requirements of the ligands. Thus, it is not likely that there exists, for any force field, a universal set of parameters for lanthanide ions, e.g., idealized M−L bond distances or L−M−L bond angles, that will allow reliable structures to be determined for all classes of lanthanide complexes using molecular mechanics. Recently, Hay reported a novel method of carrying out molecular mechanics calculations on lanthanide complexes that effectively eliminated bond angles involving the lanthanide ion.[20] Our approach is to eliminate all interactions involving the lanthanide ion by locking the donor atoms on the lanthanide surface during energy minimization, and then through an iterative procedure using the R value obtained from analysis of the LIS data as the criterion for the reliability of the structure. We will show that such an approach provides a means to accurately predict the structure of the coordination polyhedron and, to some degree, distinguish variations in M−L bond distances across the lanthanide series.

Experimental Section

The ^1H NMR spectra of solutions of all the complexes in deuterated acetonitrile (ca. 0.05 M) were recorded from 233 to 353 K on a Varian Gemini Broadband 300 MHz spectrometer. The residual proton signal from the solvent was used as an internal standard. ^{13}C spectra were obtained only for the Ln = La, Pr, Nd, Sm, Eu, and Lu complexes, using a ^{13}C resonance of the solvent as the internal standard. The analyses of LIS data were carried out using the spectra recorded at 253 K. Temperature calibration was checked using ethylene glycol and methanol samples. 2D COSY spectra (either 512 × 512 or 1024 × 1024 data points in F_1 and F_2) were recorded for the Ln = La, Pr, Nd, Sm, Eu, Yb, and Lu complexes. Attempts to obtain meaningful COSY data on the other complexes were not successful.

Longitudinal relaxation times (T_1) were measured by the inversion−recovery technique. Transverse relaxation times (T_2) were measured from the width of the peaks at half-height.

Molecular mechanics calculations were carried out on Macintosh Quadra computers using software from CAChe Scientific. The CAChe program uses Allinger's MM2 force field,[21] which has been augmented to allow minimization on metal complexes of any coordination number and geometry.

The anhydrous lanthanide trifluoromethanesulfonate (triflate) salts[22] and cyclen[23] were prepared according to procedures reported in the literature. Acetonitrile and deuterated acetonitrile (Aldrich) were distilled from P_4O_{10} prior to use.

(6) (a) Desreux, J. F. *Inorg. Chem.* **1980**, *19*, 1319. (b) Spirlet, M. R.; Rebizant, J.; Desreux, J. F.; Loncin, M. F. *Inorg. Chem.* **1984**, *23*, 359. (c) Loncin, M. F.; Desreux, J. F.; Merciny, E. *Inorg. Chem.* **1986**, *25*, 2646. (d) Brittain, H. G.; Desreux, J. F. *Inorg. Chem.* **1984**, *23*, 4459. (e) Jacques, V.; Desreux, J. F. *Inorg. Chem.* **1994**, *33*, 4048.

(7) Morrow, J. R.; Chin, K. O. A. *Inorg. Chem.* **1993**, *32*, 3357.

(8) Morrow, J. R.; Amin, S.; Lake, C. H.; Churchill, M. R. *Inorg. Chem.* **1993**, *32*, 4566.

(9) Chin, K. O. A.; Morrow, J. R.; Lake, C. H.; Churchill, M. R. *Inorg. Chem.* **1994**, *33*, 656.

(10) Aime, S.; Botta, M.; Ermondi, G. *Inorg. Chem.* **1992**, *31*, 4291.

(11) Kang, S. I.; Ranganathan, R. S.; Emswiler, J. E.; Kumar, K.; Gougoutas, J. Z.; Malley, M. F.; Tweedle, M. F. *Inorg. Chem.* **1993**, *32*, 2912.

(12) Kumar, K.; Tweedle, M. F. *Inorg. Chem.* **1993**, *32*, 4193.

(13) Frey, S. T.; Chang, C. A.; Carvalho, J. F.; Varadarajan, A.; Schultze, L. M.; Pounds, K. L.; Horrocks, W. D. *Inorg. Chem.* **1994**, *33*, 2882.

(14) Aime, S.; Anelli, P. L.; Botta, M.; Fedeli, F.; Grandi, M.; Paoli, P.; Uggeri, F. *Inorg. Chem.* **1992**, *31*, 2422.

(15) Kumar, K.; Chang, C. A.; Francesconi, L. C.; Dischino, D. D.; Malley, M. F.; Gougoutas, J. Z.; Tweedle, M. F. *Inorg. Chem.* **1994**, *33*, 3567.

(16) Toth, E.; Brücher, E.; Lazar, I.; Toth, I. *Inorg. Chem.* **1994**, *33*, 4070.

(17) Aime, S.; Barbero, L.; Botta, M.; Ermondi, G. *J. Chem. Soc. Dalton Trans.* **1992**, 225.

(18) See ref 7−9 for other studies of lanthanide complexes derived from neutral analogues of DOTA.

(19) Geraldes, F. G. C. C.; Sherry, A. D.; Kiefer, G. E. *J. Magn. Reson.* **1992**, *97*, 290.

(20) Hay, B. *Inorg. Chem.* **1991**, *30*, 2876.

(21) Allinger, N. L. *J. Am. Chem. Soc.* **1977**, *99*, 8127.

(22) Forsberg, J. H.; Spaziano, V. T.; Balasubramanian, T. M.; Liu, G. K.; Kinsley, S. A.; Duckworth, C. A.; Poteruca, J. J.; Brown, P. S.; Miller, J. L. *J. Org. Chem.* **1987**, *52*, 1017.

(23) Atkins, T. J.; Richman, J. E.; Oettle, W. F. *Org. Synth.* **1978**, *58*, 86.

The elemental analysis was performed by Galbraith Laboratories, Knoxville, TN.

1,4,7,10-Tetrakis(*N,N*-diethylacetamido)-1,4,7,10-tetraazacyclododecane (1). The ligand was prepared by mixing cyclen (1.80 g, 10.5 mmol) with 2-chloro-*N,N*-diethylacetamide (7.11 g, 53 mmol) and excess potassium hydrogen carbonate (5.8 g, 57 mmol) in 60 mL of anhydrous methanol and heating the mixture at reflux under a nitrogen atmosphere for 5 h. The reaction mixture was filtered, and the solvent was removed from the filtrate under vacuum on a rotary evaporator. The resulting solid, which contained potassium ion, presumably due to coordination to the ligand, was added to 45 mL of chloroform, and the mixture was heated at reflux for 24 h to effect precipitation of potassium chloride. The mixture was then filtered, the filtrate was placed on a rotary evaporator, and the solvent was removed under vacuum, yielding a reddish oil. The round-bottom flask containing the oil was placed into a dry ice–acetone bath. When the oil became hard, diethyl ether was added, and the mixture was stirred with a glass rod to initiate precipitation of the ligand as a white solid. If no precipitate formed, the mixture was placed back in the cold bath and the procedure was repeated. Once a solid was obtained, it was collected by filtration under suction and then washed with cold diethyl ether. The solid was kept under vacuum at 80 °C for 2 days (15% yield, mp = 116 °C dec). Anal. Calcd for $C_{32}H_{64}N_8O_4$: C, 61.56; H, 10.33, N, 18.02. Found: C, 61.01; H, 10.62; N, 17.68.

Lanthanide Complexes Derived from 1. Ln[1](CF₃SO₃)₃. The complexes (Ln = La, Pr, Nd, Sm, Eu, Tb, Dy, Ho, Er, Tm, Yb, and Lu) were prepared by mixing **1** (0.110 g, 50.0 mmol) with a 10% molar excess of the anhydrous lanthanide triflate salt in 10 mL of anhydrous acetonitrile under a nitrogen atmosphere in a glovebox. The mixtures were then heated at reflux for 48 h under nitrogen. The reaction mixtures were filtered to remove the excess triflate salt, and then the solvent was removed from the filtrates on a rotary evaporator, yielding amorphous solid residues. Since **1** was determined to be hygroscopic, the solid residues were kept under vacuum at 80 °C for 48 h to remove any residual water prior to obtaining the NMR spectra. The purity of each complex was confirmed by NMR.

The SHIFT ANALYSIS Program and Permutation of Pseudocontact Shifts. Following the procedure of Kemple et al.,[4] we have written a computer program, SHIFT ANALYSIS, for the Macintosh II series and Quadra computers, taking advantage of the graphical interface of these computers. Kemple included the option of using contact shifts as fitting parameters in his approach; thus, we also included this as an option in our program.

The measured shifts are written as linear combinations of the five components of the susceptibility tensor χ (the pseudocontact shifts) and of the assumed number of contact shifts,

$$\delta_\alpha = \sum_{j=1}^{m} G_{\alpha j} a_j \quad \alpha = 1, 2, ..., n \quad (5)$$

with δ_α being the measured shift in ppm for atom α in a molecule with n atoms;

$$a_1 = \chi_{zz} - \frac{1}{3}\mathrm{Tr}\chi \quad a_2 = \chi_{xx} - \chi_{yy} \quad a_3 = \chi_{xy} \quad a_4 = \chi_{xz}$$
$$a_5 = \chi_{yz} \quad (6)$$

$a_6, a_7, ... a_m$ are the contact shifts;

$$G_{\alpha 1} = \left(\frac{3z^2 - r^2}{r^5}\right)_\alpha \quad G_{\alpha 2} = \left(\frac{x^2 - y^2}{r^5}\right)_\alpha$$
$$G_{\alpha 3} = \left(\frac{4xy}{r^5}\right)_\alpha \quad G_{\alpha 4} = \left(\frac{4xz}{r^5}\right)_\alpha \quad G_{\alpha 5} = \left(\frac{4yz}{r^5}\right)_\alpha \quad (7)$$

where the Cartesian coordinates of atom α relative to the location of a paramagnetic ion are used in place of the more usual spherical coordinates (see eq 3) and $G_{\alpha 6}, G_{\alpha 7}, ..., G_{\alpha m}$ are all zero if atom α has no contact shift or are all zero except for the one (having the value 1) associated with the desired contact shift. In the principal magnetic axis system, $a_3 = a_4 = a_5 = 0$, and for axial symmetry, $a_2 = 0$. The pseudocontact shifts depend only on the susceptibility anisotropy (the

traceless part of the tensor). A linear least-squares analysis minimizes

$$R^2 = \frac{\displaystyle\sum_{\alpha=1}^{n} \frac{1}{\sigma_\alpha^2}\left(\sum_{j=1}^{m} G_{\alpha j} a_j - \delta_\alpha\right)^2}{\displaystyle\sum_{\alpha=1}^{n} \frac{\delta_\alpha^2}{\sigma_\alpha^2}} \quad (8)$$

by variation of the a_j parameters. The σ_α are the standard deviations of the measured shifts. A standard analysis finds

$$a_j = \sum_{k=1}^{m} (\mathbf{B}^{-1})_{jk} C_k \quad (9)$$

where $\mathbf{B}$ is the matrix whose elements are

$$B_{jk} = \sum_{\alpha=1}^{n} \frac{1}{\sigma_\alpha^2} G_{\alpha j} G_{\alpha k} \quad (10)$$

and where

$$C_k = \sum_{\alpha=1}^{n} \frac{1}{\sigma_\alpha^2} G_{\alpha k} \delta_\alpha \quad (11)$$

Substitution of eq 9 in eq 8 yields $R^2 = 1 - Q$, where

$$Q = \sum_{j=1}^{m}\sum_{k=1}^{m} (\mathbf{B}^{-1})_{jk} C_j C_k \quad (12)$$

Substituion of eq 11 into eq 12 gives

$$Q = \sum_{\alpha=1}^{n}\sum_{\beta=1}^{n} M_{\alpha\beta}\delta_\alpha\delta_\beta \quad (13)$$

where

$$M_{\alpha\beta} = \frac{1}{\sigma_\alpha^2}\frac{1}{\sigma_\beta^2} \sum_{j=1}^{m}\sum_{k=1}^{m} (\mathbf{B}^{-1})_{jk} G_{\alpha j} G_{\beta k} \quad (14)$$

It is often the case that an unequivocal assignment of the peaks in the spectrum is not possible. It is noted that the $M_{\alpha\beta}$ values are independent of the observed pseudocontact shifts, δ_α, but dependent on the standard deviations σ_α (eq 14); thus, Q has a quadratic dependence on the pseudocontact shifts. If one now takes the standard deviations σ_α to be the same for all shifts, the $M_{\alpha\beta}$ are independent of permutations of the pseudocontact shifts. Thus, a reassignment of the observed pseudocontact shifts corresponds to a certain permutation of the shifts in eq 13. Presumably that permutation which maximizes Q and thereby minimizes R^2 ($R^2 = 1 - Q$) will give the optimal assignment of observed pseudocontact shifts to their respective atoms. The simplicity of eq 13 allows these calculations to be done rapidly on a personal computer. For example, on a computer with a floating-point processor, the calculation for eight atoms (40 320 permutations) takes less than 1 min; the calculation for nine atoms (362 880 permutations) takes less than 10 min. Unfortunately, when there are a large number of atoms involved, the time required to do the calculation, even on a supercomputer, becomes prohibitive.

When no computationally feasible optimal procedure exists, interest must focus on sub-optimal procedures. One of us (R.M.D.) independently developed a sub-optimal procedure, which we termed the JOLT method, with the essential features described earlier by Burkard and Stratmann.[24] The fundamental idea is to generate a random permutation of the pseudocontact shifts, which gives a starting value for Q. A small

(24) Burkard, R. E.; Stratmann, K. *Naval Research Logistics Quarterly* **1978**, *25*, 129.
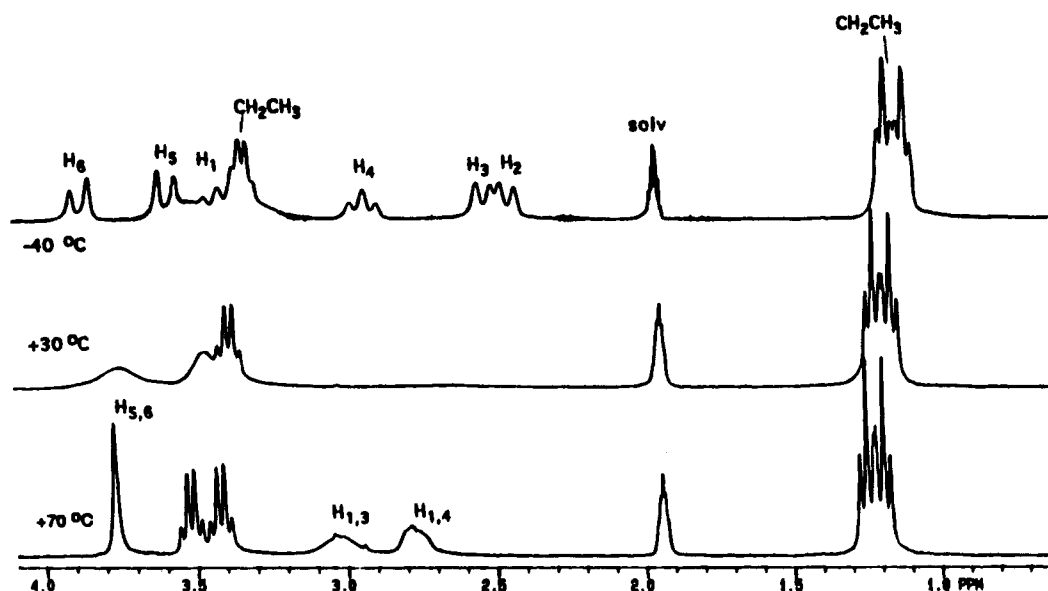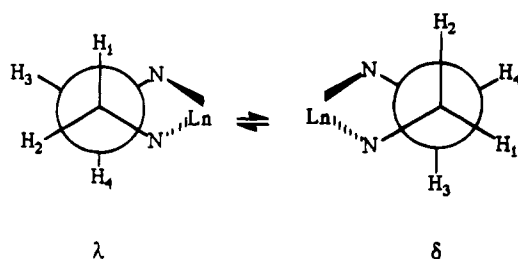
Figure 1. Variable-temperature ^1H NMR spectra of solutions of the lanthanum complex in deuterated acetonitrile.
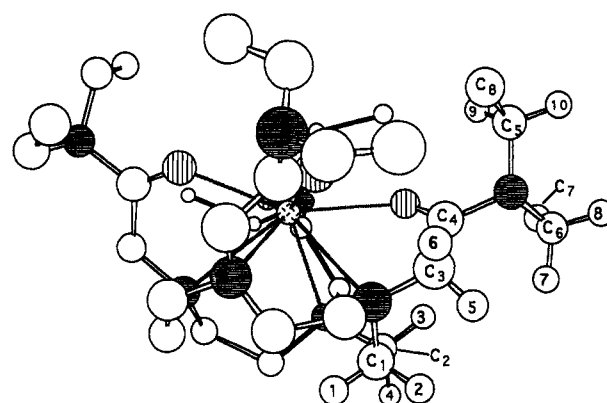
Scheme 1

Figure 2. Model of the complex showing the numbering scheme for carbon and hydrogen atoms. Symmetry-related hydrogen atoms are not shown for clarity. Circles with horizontal cross-hatching denote N atoms; circles with vertical cross-hatching denote O atoms.

change is then made in the permutation, and Q is recalculated. If the new Q is larger, the new permutation and the new Q_{max} are accepted; if not, they are rejected. The process is repeated until, after a certain number of trials, Q_{max} does not change. Then another random permutation (the JOLT) is generated, and the process is repeated. With a sufficient number of random permutations, one hopes to obtain an optimal Q_{max}.

To establish the efficacy of the JOLT method, pseudocontact shifts were calculated from randomly generated position coordinates for 24 atoms and susceptibility tensor components. Using a Gaussian distribution of standard deviations, the optimal R^2 values were determined. The shifts were then given a random permutation, and the JOLT method was applied to reassign the shifts to the correct atoms. With a run defined as 300 JOLTS, the results for 100 runs revealed that the optimal R^2 value was attained in each run, usually several times (the minimum number of JOLTS giving the optimal value was 4, with a maximum of 168). The average time for 300 JOLTS on Macintosh IIfx was about 2 h.

Results and Discussion

Spectra of Diamagnetic Complexes. The ^1H spectra of the diamagnetic 1:1 lanthanum complex as a function of temperature are shown in Figure 1. The spectrum at -40 °C reveals that the $\lambda \rightleftharpoons \delta$ interchange between the two enantiomeric conformers of each ethylenediamine chelate ring of the macrocycle (Scheme 1) is slow on the NMR time scale. The equatorial proton (H_2 and H_3 in the λ conformation) resonances appear as broad doublets due to geminal coupling ($^1J = 15$ Hz) at δ 2.43 (La^{3+}), 2.67 (Lu^{3+}) and δ 2.52 (La^{3+}), 2.81 (Lu^{3+}), respectively (all chemical shifts are in ppm relative to TMS). The trans pair of axial protons (H_1 and H_4) reveal vicinal coupling in addition to geminal coupling and thus appear as broad triplets ($^1J \approx {}^3J \approx$ 13 Hz) at δ 3.41 (La^{3+}), 3.36 (Lu^{3+}) and δ 2.93 (La^{3+}), 2.96 (Lu^{3+}), respectively (the assignment of the downfield peak to

H_1 is based on its closer proximity to the Ln^{3+} ion). The nonequivalence of the methylene hydrogen atoms H_5 and H_6 (see Figure 2 for atom assignments) of the pendant acetamide arms (AB pattern at δ 3.58 (La^{3+}), 3.81 (Lu^{3+}) and δ 3.87 (La^{3+}), 4.06 (Lu^{3+}), $^1J \approx$ 17 Hz), verifies the structurally rigid nature of the complex at lower temperatures. As expected in an amide, the methyl groups are nonequivalent, appearing as triplets ($^3J =$ 7.0 Hz) at δ 1.11, 1.17 (La^{3+}) and δ 1.24, 1.15 (Lu^{3+}). The major difference in the spectra of the lanthanum and lutetium complexes occurs in the region of the methylene resonances of the ethyl group. In the temperature range 30 to -40 °C, the spectrum of the lanthanum complex reveals a broad quartet ($^3J =$ 7.0 Hz) centered at δ 3.32 (at -40 °C), corresponding to the two nonequivalent methylene groups, which are coincidentally nearly isochronous (at 70 °C, the two quartets are observed at δ 3.42 ($^3J =$ 7.2 Hz) and δ 3.52 ($^3J =$ 7.4 Hz)). However, the spectrum of the lutetium complex gives one quartet at δ 3.23 ($^3J =$ 7 Hz), but the geminal protons of the other methylene group are nonequivalent, giving rise to sextets (overlapping quartet of doublets, with $^1J = \sim 14$ Hz and $^3J = \sim 7$ Hz) centered at δ 2.98 and 3.47. The latter observation suggests that sufficient steric hindrance exists within at least one of the sets of symmetry-equivalent ethyl groups to hinder rotation around the $N-CH_2CH_3$ bond. (As noted below, the spectra of all the paramagnetic chelates reveal that the geminal
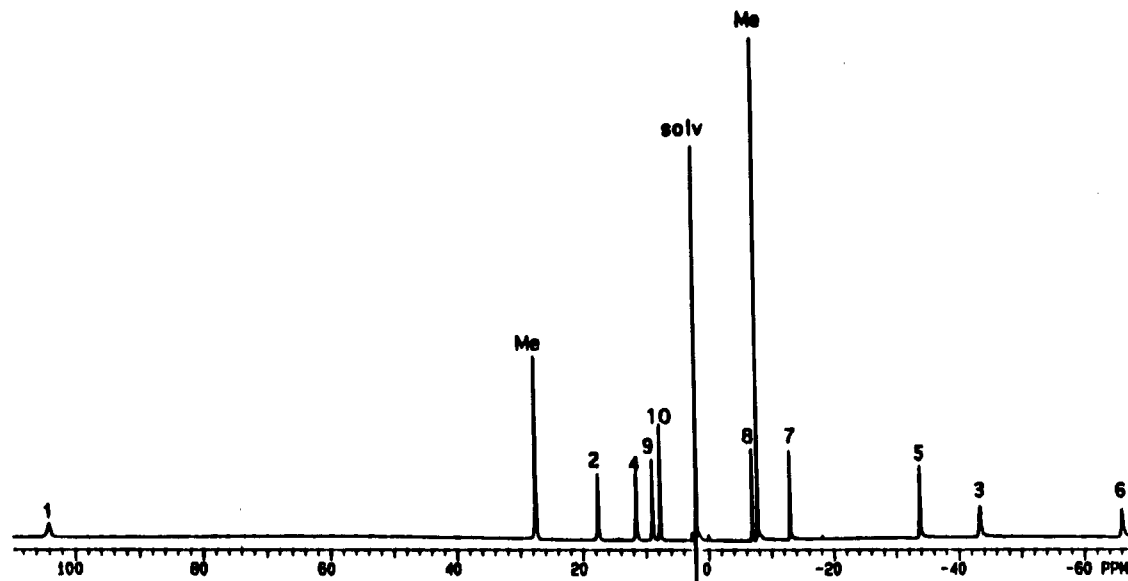
Figure 3. ^{1}H spectrum of the ytterbium complex derived from **1**. See Figure 2 for numbering scheme used for peak assignments.

hydrogen atoms of both methylene groups are nonequivalent.) The vicinal and geminal couplings reported above are confirmed by cross peaks observed in the 2D COSY spectra for the lanthanum and lutetium complexes.

As the temperature is increased, the interchange between the λ and δ conformers exchanges H$_1$ with H$_3$ and H$_2$ with H$_4$, resulting in two broad, unresolved peaks (AA′BB′ pattern) at δ 3.03 and 2.77, respectively, in the spectrum of the lanthanum complex. At the same time, the methylene resonances of the pendant arms (H$_5$ and H$_6$) become equivalent, appearing as a singlet at δ 3.78. However, the observation of separate signals for the two methyl and methylene resonances for the ethyl group indicate that rotation about the C−N (amide) bond remains hindered at 70 °C.

The ^{13}C spectra of the diamagnetic chelates confirm the structurally rigid nature of the complexes at room temperature, δ (ppm), La^{3+}, Lu^{3+}: C$_1$, 50.3, 49.6; C$_2$, 55.2, 55.4; C$_3$, 58.3, 58.3; C$_4$, 173.4, 174.8; C$_5$, 43.3, 43.7; C$_6$, 44.1, 44.2; C$_7$, 14.4, 13.6; C$_8$, 13.4, 12.4 (see Figure 2 for atom assignments). As the temperature is increased, the two resonances assigned to the macrocyclic ring carbon atoms coalesce. Complete line shape analysis[25] was carried out on spectra obtained over the temperature range 293 to 333 K. A plot of k/T vs $1/T[k = (k_bT/h) \exp(\Delta S^\ddagger/R - \Delta H^\ddagger/RT)]$ yields the activation parameters ($\Delta G^\ddagger = 58.8$ kJ/mol, $\Delta H^\ddagger = 52.1$ kJ/mol, and $\Delta S^\ddagger = -22.5$ J/K mol; $k = 300$ s^{-1} at 298 K). Comparison of these data with those obtained for [LaDOTA]$^-$ ($\Delta G^\ddagger = 60.7$ kJ/mol at 300 K) reveals that increasing the steric bulk of the pendant arms has little effect on the dynamics of interconversion between the λ and δ conformations of the macrocyclic ring.[6a]

Spectra of Paramagnetic Complexes. The ^{1}H NMR spectrum of solutions of each paramagnetic 1:1 chelate (Ln = Pr, Nd, Sm, Eu, Tb, Dy, Ho, Er, Tm, and Yb) in deuterated acetonitrile revealed 12 peaks, consistent with a sterically rigid, eight-coordinate complex having a C$_4$ symmetry axis, suggesting that the donor atoms are located at the vertices of a square antiprism. The spectrum of the ytterbium complex is presented in Figure 3. In addition to the nonequivalencies noted above for the diamagnetic complexes, each of the methylene protons (H$_7$, H$_8$, H$_9$, and H$_{10}$) of the ethyl groups are also nonequivalent, indicating that sufficient steric hindrance exists between the

pendant arms to restrict free rotation about the N−C(5) and N−C(6) bonds. The assignments given in Table 1 were obtained using the JOLT method (*vide supra*). Due to free rotation, the protons of the methyl group were not included in the LIS analysis, and therefore, their assignments are not included in Table 1.

2D COSY spectra were obtained for Ln = Pr, Nd, Sm, Eu, and Yb. The spectrum of the ytterbium complex is presented in Figure 4. Cross peaks are observed for each pair of geminal protons. In addition to geminal coupling, the methylene protons of the ethyl group also reveal cross peaks to the methyl protons (see inset in Figure 4 showing the cross peaks involving H$_9$, H$_{10}$, and one of the methyl groups), which allows H$_7$, H$_8$, H$_9$, and H$_{10}$ to be distinguished from the other, equally intense proton resonances assigned to the macrocyclic ring (H$_1$−H$_4$) and pendant arm methylene hydrogen atoms (H$_5$ and H$_6$). Cross peaks were not observed in the COSY spectra of the other heavy, paramagnetic chelates, presumably due to effective transverse relaxation.[26]

The ^{13}C spectra revealed eight peaks, consistent with a complex having C$_4$ symmetry. The LIS values for the Ln = Pr, Nd, Sm, and Eu complexes are presented in Table 2. Due to line broadening, ^{13}C spectra were not obtained for complexes derived from the smaller paramagnetic metal ions (Tb−Yb).

Each complex has two independent structural features that are sources of chirality for the complexes. The pendant arms may be oriented around the C$_4$ symmetry axis of the complex in a propeller-like manner in either a clockwise (A) or counterclockwise (B) direction (Chart 1). Secondly, as noted above, each ethylenediamine ring of the macrocycle can adopt two different conformations (λ or δ) when coordinated to the metal ion. The observation of only 12 peaks in the spectrum of each paramagnetic complex suggests that all the ethylene-diamine rings in a particular ligand molecule adopt either the λ or δ conformation and that, for a given conformation of the macrocycle, the pendant arms are rotated in only one direction, i.e., the complex exists as a single pair of enantiomers in solution. If the ethylenediamine rings were to adopt both λ and δ conformations within a single ligand molecule, then diastereomers would be observed, giving rise to a set of 12

(25) Forsberg, J. H.; Dolter, T. J.; Carter, A. M.; Singh, D.; Aubuchon, S. A.; Timperman, A. T.; Ziaee, A. *Inorg. Chem.* **1992**, *31*, 5555.

(26) Intensity of a cross peak is proportional to exp $-t_1/T_2$ sin πJt_1, where t_1 is the evolution time in the second dimension, J is the coupling constant, and T_2 is the transverse relaxation time.[27]

Table 1. ¹H LIS Data for Lanthanide Complexes Derived from 1[a]

Ln		H 1	2	3	4	5	6	7	8	9	10	R
Pr	LIS$_{obsv}$	−47.7	−5.3	16.6	−2.3	14.7	28.6	8.9	6.7	1.2	3.4	0.051
	LIS$_{calc}$	−47.5	−5.8	15.2	−1.3	15.1	29.4	9.6	6.4	−0.9	2.4	
	$\delta_c{}^b$	−0.9	4.9	0.6	6.3	3.4	0.4	0.2	0.4	0.0	−0.3	
Nd	LIS$_{obsv}$	−22.2	2.4	7.8	5.2	9.3	11.7	4.1	3.3	9.7	1.9	
	LIS$_{calc}$	−21.5	2.8	7.2	6.1	10.2	13.3	4.4	3.2	−0.3	0.7	0.104
	$\delta_c{}^b$	−1.3	7.4	0.9	9.4	5.1	0.7	0.3	0.6	0.1	−0.5	
Sm	LIS$_{obsv}$	−3.89	−0.94	1.30	−0.80	1.10	2.55	0.68	0.51	−0.09	0.48	
	LIS$_{calc}$	−3.91	−0.90	1.29	−0.67	1.02	2.59	0.81	0.50	0.00	0.23	0.066
	$\delta_c{}^b$	1	−0.05	−0.01	−0.06	−0.03	0.00	0.00	0.00	0.00	0.00	
Eu	LIS$_{obsv}$	21.6	−8.5	−8.2	−12.5	−13.6	−13.4	−4.1	−3.6	−0.5	−0.5	
	LIS$_{calc}$	21.0	−8.5	−8.0	−13.1	−14.0	−14.1	−4.1	−3.6	−0.5	−0.5	0.062
	$\delta_c{}^b$	2.2	−12.5	−1.5	−15.9	−8.6	−1.1	−0.5	−1.0	−0.1	0.8	
Tb	LIS$_{obsv}$	−454.1	−118.4	166.5	−113.6	114.5	315.6	86.6	61.2	−1.3	14.6	
	LIS$_{calc}$	−463.5	−117.5	150.4	−108.1	112.2	310.5	86.6	61.2	−1.3	14.6	0.037
	$\delta_c{}^b$	−7.4	−39.3	−22.4	−51.7	−33.5	−2.7	7.7	10.2	16.2	14.0	
Dy	LIS$_{obsv}$	−490.2	−112.3	190.5	−106.7	136.8	349.5	91.2	66.7	−8.3	9.9	
	LIS$_{calc}$	−504.2	−115	175.8	−102.9	132.5	336.9	103.7	61.0	−6.5	9.8	0.042
	$\delta_c{}^b$	−6.7	−35.3	−20.1	−46.4	−30.2	−2.4	6.6	9.3	14.5	12.7	
Ho	LIS$_{obsv}$	−233.3	−55.1	94.0	−53.0	62.9	163.0	42.5	30.2	−5.0	3.3	
	LIS$_{calc}$	−242.3	−57.9	86.8	−56.4	57.8	153.7	50.5	29.7	−3.6	6.6	0.058
	$\delta_c{}^b$	−5.3	−27.9	−15.9	−36.7	−23.9	−1.9	5.5	7.4	11.5	10.1	
Er	LIS$_{obsv}$	292.3	38.3	−129.0	15.2	−109.8	−208.1	−48.4	−31.4	17.3	12.2	
	LIS$_{calc}$	295.5	32.2	−124.1	11.9	−111.5	−206.1	−54.9	−26.9	19.7	7.5	0.033
	$\delta_c{}^b$	−3.6	−19.0	−10.8	−25.0	−16.2	−1.3	3.7	5.0	7.8	6.8	
Tm	LIS$_{obsv}$	789.7	105.5	−363.0	80.6	−290.1	−577.2	−134.4	−84.4	46.5	5.5	
	LIS$_{calc}$	815.6	107.3	−344.4	67.1	−283.8	−549	−156.0	−78.5	49.9	13.8	0.046
	$\delta_c{}^b$	−2.1	−10.2	−5.7	−13.4	−8.6	−0.6	2.1	2.7	4.2	5.1	
Yb	LIS$_{obsv}$	100.6	14.9	−46.4	8.7	−37.6	−70.2	−16.4	−10.3	5.6	4.4	
	LIS$_{calc}$	101.5	12.2	−43.5	6.6	−37.4	−70.6	−19.8	−9.8	6.4	2.0	0.044
	LIS$_{calc}{}^c$	99.2	12.2	−45.6	7.2	−36.8	−70.8	−21.5	−9.7	17.6	2.3	0.100
	$\delta_c{}^b$	−0.6	−3.2	−1.8	−4.2	−2.7	−0.2	0.6	0.8	1.3	1.1	

[a] LIS values in ppm. Positive shifts are to higher frequency (downfield). LIS values for Ln = Pr−Eu referenced to the lanthnanum complex; values for Ln = Tb−Yb referenced to the lutetium complex. Calculated values obtained for optimal geometries with clockwise rotation of the pendant arms about the C₄ axis (viewed from the plane of oxygen atoms) with each chelate ring of the macrocycle in the λ conformation. [b] From linear least-squares analysis of the data set using eqs 19−22. [c] Calculated for counterclockwise rotation of the pendant arms about the C₄ axis, retaining the λ conformation of each chelate ring of the macrocycle.

additional peaks in the spectrum for each diastereomer. Likewise, diastereomers would be observed if the pendant arms were to rotate in either a clockwise or a counterclockwise manner about the C₄ axis for a fixed conformation of the macrocyclic ring. Thus, it is concluded that all four ethylenediamine rings adopt the same conformation, giving rise to a single pair of enantiomers, which of course cannot be distinguished by NMR. We will show through analysis of our LIS data (*vide infra*) that the enantiomer with each ethylenediamine ring in a λ conformation prefers a clockwise rotation (A) of the pendant arms. Although each of the protons is distinguished in a spectrum recorded at room temperature, as the temperature of the solution is increased, exchange between the two enantiomers results in broadening and partial coalescence of pairs of resonances, e.g., H₁ and H₃, H₂ and H₄, H₅ and H₆, etc. A more complete description of the structure of each complex is presented in the section on refinement of structure.

Assignment of Peaks. The following strategy was developed to establish the efficacy of the JOLT procedure, which is included as an option in the SHIFT ANALYSIS program, to assign LIS values to the hydrogen atoms in each complex. Since the LIS values are not corrected for contact shifts at this stage, the analysis is initiated with the ytterbium complex, since ytterbium has the largest ratio of pseudocontact to contact shifts. Furthermore, since the peaks are not yet assigned, the LIS values were determined by assuming an average $\delta_{diamagnetic}$ value of 3.4 ppm (δ values for the Lu³⁺ complex ranged from 2.67 to 4.06 ppm).

Molecular modeling was carried out by first approximating a structure for the complex using the atomic coordinates reported

for the structure of Na[Eu(DOTA)H₂O)]·4H₂O[6b] but with the carboxyl groups replaced with N,N-diethylacetamide groups. The donor atoms were placed at the vertices of a distorted square antiprism, using distances of 2.65 and 2.40 Å for the Yb³⁺−N and Yb³⁺−O bonds, respectively. Three dihedral angles are required to define the position of the two sets of methylene hydrogen atoms of the ethyl groups: A = ∠C(5)NC(4)C(3), B = ∠C(7)C(6)NC(4), and C = ∠C(8)C(5)NC(4) (see Figure 2 for assignment of atoms). In the optimized structures (see refinement of structure), A = −141°, B = 73.5°, and C = 95° for Ln = Pr, Nd, Sm, and Eu, whereas A = −147°, B = 78.5°, and C = 62° for Ln = Tb, Dy, Ho, Er, Tm, and Yb. Energy minimization was then carried out, locking the donor atoms on the surface of the metal ion. The resulting coordinates for H₁−H₁₀ were entered into the SHIFT ANALYSIS program. The JOLT method (*vide supra*) was used to assign the LIS values to the 40 hydrogen atoms of the ligand (there are four symmetry-equivalent hydrogen atoms in each set labeled H₁−H₁₀; therefore, each of the ten LIS values is randomly entered in the program four times). Criteria for a correct assignment are that the symmetry-related protons are assigned the same LIS value, that the LIS values for geminal protons are consistent with 2D COSY spectra (*vide supra*), and that the assignments are consistent with the longitudinal (T₁) and transverse (T₂) relaxation times (Table 3), which reveal an r⁻⁶ dependency on the proton−metal distance. The assignments reported in Table 1 are also consistent with those reported by Desreux et al.[6a] for the analogous [Yb(DOTA)]⁻ complex. The calculations were carried out using the full expression given in eq 3 (five-parameter fit). The results show that the complex is axially
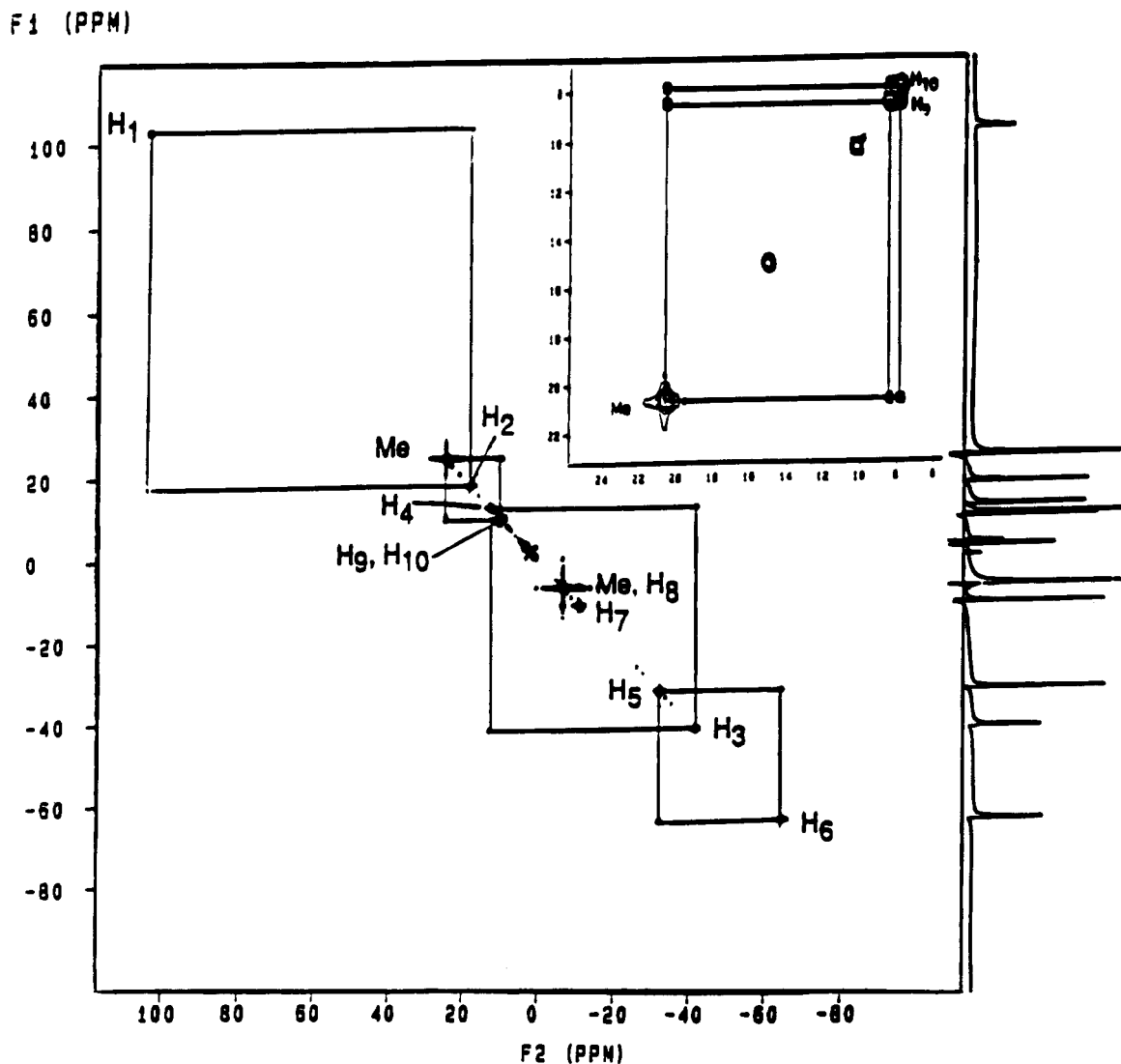
Figure 4. 2D COSY spectrum of the ytterbium complex derived from **1**. Inset shows expansion of the region of 8 to 24 ppm. See Figure 2 for numbering scheme used for peak assignments.

Table 2. LIS Values and Contact Shifts for Selected ^{13}C Nuclei (in ppm)

	Pr		Nd		Sm		Eu	
C	LIS^a	δ_c	LIS^a	δ_c	LIS^a	δ_c	LIS^a	δ_c
C(1)	−51.6	−15.2	−38.8	−18.5	−1.58	+1.07	+50.5	+27.2
C(2)	−27.3	−15.5	−26.5	−19.9	+0.40	+1.26	+36.4	+29.3
C(3)	+17.8	−17.6	−5.6	−25.3	+3.58	+0.91	+19.8	+45.2
C(4)	+19.7	−34.0	−8.6	−38.5	+6.15	+2.11	+10.2	+53.1

^{a} Referenced to the lanthanum complex.

Chart 1

(A)   (B)
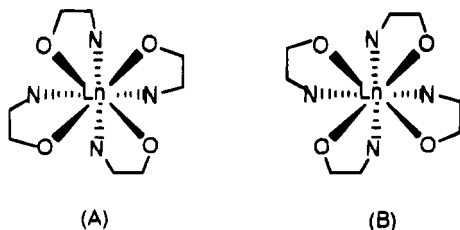
symmetric, e.g., for the ytterbium complex, $\chi_{xy} = 0.10$, $\chi_{xz} = 0.07$, $\chi_{yz} = -0.07$, $\chi_{xx} = \chi_{yy} = -1969$ VVk/mol[28]) ($\chi_{zz} - \text{Tr}\chi = 3269$ VVk/mol). Furthermore, diagonalization of the tensor

provides a set of Euler angles that relate the principal magnetic axis system to the molecular coordinate system. The results for ytterbium are typical of each complex: $\theta = 0.001°$ (tilt of C_4 symmetry axis from the principal magnetic z axis), $\phi = 45°$, and $\gamma = -72°$. The combined values of ϕ and γ indicate that the principal magnetic x and y axes are rotated $-27°$ from the molecular x and y axes (the molecular x and y axes are along the projection of the Ln—N bonds in a plane containing the Ln^{3+} ion, which is perpendicular to the C_4 symmetry axis). The assignments of H$_1$—H$_{10}$ in the spectra of the other complexes can be based on the observation that most spectra reveal the same pattern of peaks as observed in the spectrum of the ytterbium complex. However, it is interesting to note that, with the exception of the neodymium and europium complexes, which have the largest contact shift to pseudocontact shift ratios, the JOLT method also gave a consistent set of assignments for each of the complexes without correcting the LIS values for a contact shift.

Separation of Contact and Pseudocontact Components of the LIS. Before attempting to refine the geometry of the complex, it is necessary to separate the contact shift from the observed LIS values. The most general method for separating the LIS into contact and pseudocontact components was

(27) Derome, A. E. *Modern NMR Techniques for Chemistry Research*; Pergamon Press: Oxford, 1987, p 222.

(28) 1 van Vleck (VVk) = 10^{-6} cgs.[29]

Table 3. Longitudinal (T_1) and Transverse (T_2) Relaxation Times of the Protons in the Praseodymium and Ytterbium Complexes Derived from **1**[a]

Ln		1	2	3	4	5	6	7	8	9	10
						H					
Pr	$T_1 \times 10^2$ (s)	2.35	3.97	0.86	3.43	2.35	0.66	9.74	11.8	6.28	5.41
	$T_2 \times 10^3$ (s)	2.97	4.70	3.57	6.15	4.44	3.05	5.11	7.56	6.07	9.68
	$r(\text{Å})^b$	0.390	0.461	0.379	0.461	0.454	0.384	0.558	0.756	0.452	0.605
Yb	$T_1 \times 10^2$ (s)	0.30	1.14	0.55	1.13	1.61	0.60	5.89	7.40	1.73	3.57
	$T_2 \times 10^4$ (s)	2.52	1.04	0.95	1.26	2.73	2.07	6.22	0.96	1.56	1.70
	r (Å)^b	0.363	0.435	0.366	0.437	0.426	0.359	0.542	0.634	0.459	0.584

[a] T_1 and T_2 values ±6% error. [b] Proton metal distances were determined using the CAChe molecular modeling program and correspond to the values obtained in the optimized structures.

introduced by Reilley et al.[30] On the basis of a theoretical approach developed by Bleaney,[31] δ_{pc} is expressed as

$$\delta_{pc} = C_j G_i \qquad (15)$$

where C_j are constants (Bleaney factors) characteristic of each Ln^{3+} ion and G_i, the geometric factor for the ith nucleus, is expressed as

$$G_i = (1/r^3)[C(3\cos^2\theta - 1) + C'(\sin^2\theta\cos 2\phi)] \qquad (16)$$

where C and C' are constants which contain the crystal field coefficients $2A_2^0\langle r^2\rangle = B_0^2$ and $2A_2^2\langle r^2\rangle = B_2^2$, respectively. The crystal field coefficients are assumed to be constant for an isostructural series of lanthanide complexes. In the case of axial symmetry, $C' = 0$. δ_c may be expressed as

$$\delta_c = F_i\langle S_z\rangle_j \qquad (17)$$

where F_i represents the collection of constants in eq 2 for the ith nucleus and $\langle S_z\rangle_j$ is a metal-dependent parameter as previously defined. Since the LIS is the sum of the contact and pseudo contact components, eqs 15 and 17 can be combined to give

$$(LIS)_i/\langle S_z\rangle_j = [C_jG_i/\langle S_z\rangle_j] + F_i \qquad (18)$$

Thus, for a series of isostructural complexes, a plot of $(LIS)_i/\langle S_z\rangle_j$ vs $C_j/\langle S_z\rangle_j$ should be linear, with an intercept equal to F_i. Representative plots of $LIS_i/\langle S_z\rangle_j$ vs $C_j/\langle S_z\rangle_j$ are presented in Figure 5. With the exception of samarium, the $\langle S_z\rangle$ values used in these plots were those reported by Pinkerton et al.[3] As noted by Pinkerton,[3] the $\langle S_z\rangle$ value for samarium is extremely sensitive to temperature. Using the expression given by Golding and Halton,[2] with $\xi = 1176$ cm^{-1},[32] we calculated $\langle S_z\rangle = 0.0278$ at 253 K. With the exception of the thulium values, the plots are reasonably linear, with no apparent break in the middle of the series, as observed by others.[19,33] However, as a consequence of the lanthanide contraction, small variations in the geometric factors for each atom in the ligand are expected across the series.[33] Thus, the intercepts and corresponding contact shifts reported in Table 4 were obtained by separate least-squares analyses of the data obtained for the larger (Ln = Pr−Eu) and smaller ions (Tb−Yb).[34] The intercepts are close to zero (Table 4), verifying that the LIS data are dominated by pseudocontact shifts. Unfortunately, in most cases, the error limits are
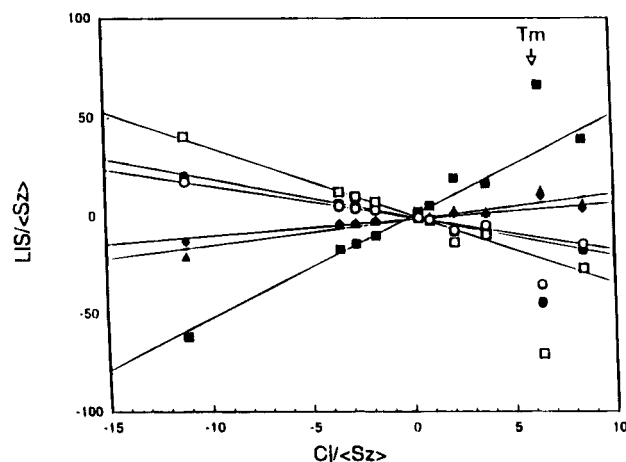

Figure 5. Plots for determining contact shifts according to eq 18. ■ = H_1, ▲ = H_2, ● = H_3, ⬤ = H_4, ○ = H_5, □ = H_6.

relatively large compared to the value of the intercepts. For ions with large values of $\langle S_z\rangle$, e.g., Tb(31.8), Dy(28.5), Ho-(22.6), a relatively large error in the intercept leads to a relatively large uncertainty in the calculated contact shifts. This uncertainty in the contact shift becomes particularly important for atoms with small geometric factors, i.e., atoms having small pseudocontact shifts, since the contact component of the LIS may become dominant.

Although Bleaney's approximation of expressing the magnetic anisotropy in terms of ligand field parameters of the second degree appears valid except at low temperatures, i.e., less than 200 K,[35] the assumption that the crystal field parameters are independent of the lanthanide ion may not be valid.[36] Variations in the ligand field parameters are expected in solution, since the Ln^{3+}−donor atom bond distances decrease as a result of the lanthanide contraction. Thus, the linearity observed in these plots may be fortuitous due to either small changes in the crystal field coefficients and geometric factors or the fact that the variation of one parameter cancels the effect of the variation of the other parameter.

Given the assumptions inherent in this separation process, we sought an alternative procedure for separating the contact component of the LIS. If we write δ_{ij} as the LIS shift for the ith nucleus on the jth metal, for axial symmetry,

$$\delta_{ij} = G_iA_j + F_i\langle S_z\rangle_j \qquad (19)$$

where G_i is the geometric factor for the ith proton and A_j represents $\chi_{zz}^j - \text{Tr}\chi^j$ for the jth metal. The idea is to find a set of optimal values of A_j, G_i, and F_i that minimize R (eq 4) for the resulting matrix of $i \times j$ simultaneous equations. We can show (see Appendix) that there exist linear transformations (eqs

(29) Horrocks, W. D.; Hall, D. D. *Inorg. Chem.* **1971**, *10*, 2368.
(30) Reilley, C. N.; Good, B. W.; Allendoerfer, R. D. *Anal. Chem.* **1976**, *48*, 1446.
(31) (a) Bleaney, B. *J. Magn. Reson.* **1972**, *8*, 91. (b) Bleaney, B.; Dobson, C. M.; Levine, B. A.; Martin, R. B.; Williams, R. J. P.; Xavier, A. V. *J. Chem. Soc., Chem. Commun.* **1972**, 791.
(32) Carnall, W. T.; Goodman, G. L.; Rajnak, K.; Rana, R. S. *J. Chem. Phys.* **1989**, *90*, 3443.
(33) Peters, J. A. *J. Magn. Reson.* **1986**, *68*, 240.
(34) The thulium data were not included in the least-squares analyses.

(35) Stout, E. W.; Gutowsky, H. S. *J. Magn. Reson.* **1976**, *24*, 389.
(36) Reuben, J. *J. Magn. Reson.* **1982**, *50*, 233.

Table 4. Geometric Factors and F_i Values for Complexes Derived from **1**

| | H_i | | | | | | | | | |
	H_1	H_2	H_3	H_4	H_5	H_6	H_7	H_8	H_9	H_{10}
$F_i(\text{Pr}-\text{Eu})^a$	-1.56 ± 1.2	-2.13 ± 0.3	0.39 ± 0.4	-2.50 ± 0.2	-0.19 ± 0.5	1.55 ± 0.9	0.20 ± 0.2	0.10 ± 0.1	-0.04 ± 0.9	0.62 ± 0.3
$F_i(\text{Tb}-\text{Yb})^a$	0.56 ± 0.4	-0.84 ± 0.5	-0.89 ± 0.9	-1.37 ± 0.4	-1.19 ± 0.7	-0.43 ± 1.7	0.12 ± 0.4	0.21 ± 0.3	0.41 ± 0.09	0.63 ± 0.09
$F_i(\text{Pr}-\text{Eu})^{b,c}$	0.30	-1.67	-0.20	-2.12	-1.15	-0.15	-0.1	-0.13	-0.01	0.10
$F_i(\text{Tb}-\text{Yb})^{b,d}$	-0.25	-1.24	-0.70	-1.63	-1.05	-0.07	0.25	0.33	0.51	0.44
$G_i \times 10^3$ $(\text{Å}^{-3})^{b,c}$ (Pr$-$Eu)	27.9	5.9	-8.79	4.34	-7.78	-19.1	-5.80	-3.52	1.26	-0.72
$G_i \times 10^3$ $(\text{Å}^{-3})^e$ (Pr$-$Eu)	27.9	6.16	-9.50	5.10	-6.62	-16.6	-5.20	-3.76	-0.67	-2.30
$G_i \times 10^3$ $(\text{Å}^{-3})^{b,d}$ (Tb$-$Yb)	31.1	5.01	-12.3	3.48	-10.3	-21.4	-6.30	-3.28	2.10	0.53
$G_i \times 10^3$ $(\text{Å}^{-3})^e$ (Tb$-$Yb)	31.1	4.83	-13.6	3.80	-10.8	-22.4	-5.40	-3.50	1.50	0.15

[a] Obtained by the method of Reilley et al.[30] [b] Obtained using the method of linear least-squares analysis (eqs 19–22) of the data normalized to the geometric factor for H_1. [c] Normalized to the anisotropy parameter for the praseodymium complex. [d] Normalized to the anisotropy parameter for the ytterbium complex. [e] Obtained using the SHIFT ANALYSIS program.

Table 5. Values of $\chi_{zz} - \frac{1}{3}\text{Tr}\chi$ (VVk/mol[28])

| | Ln[a] | | | | | | | | | |
	Pr	Nd	Sm	Eu	Tb	Dy	Ho	Er	Tm	Yb
$\chi_{zz} - \frac{1}{3}\text{Tr}\chi^b$	-1690	-729	-141	684	-15100	-16200	-7790	9960	25800	3250
$\chi_{zz} - \frac{1}{3}\text{Tr}\chi^c$	-1690	-730	-143	703	-14300	-15600	-7400	9370	25700	3250

[a] Values normalized to the geometric factor of H_1 and the $\chi_{zz} - \frac{1}{3}\text{Tr}\chi$ values of Pr (Ln = Pr, Nd, Sm, and Eu) or Yb (Ln = Tb, Dy, Ho, Er, Tm, and Yb). [b] Using the SHIFT ANALYSIS program. [c] Linear least-squares analysis of the data set (eqs 19–22).

20–22) dependent on two continuous parameters (a,c), which leave the right-hand side of eq 19 invariant.

$$G_i' = aG_i \tag{20}$$

$$F_i' = F_i + cG_i \tag{21}$$

$$A_j' = \frac{1}{a}A_j - \frac{c}{a}\langle S_z \rangle_j \tag{22}$$

Consequently, any fitting method, such as least-squares, will give an infinite number of solution sets for each of the variables A_j, G_i, and F_i. However, if values are assigned to any two of the variables, say $G_1 = G_1^\circ$ (geometric factor for H_1) and $A_1 = A_1^\circ$ ($A_1^\circ = \chi_{zz} - \frac{1}{3}\text{Tr}\chi$ for metal 1), then the parameters a and c are determined, and any solution set $(G_i', F_i'$ and $A_j')$ can be brought by the linear transformations (eqs 20–22) to the set that is scaled to G_1° and A_1°, namely G_i°, A_j°, and F_i°. The value of G_1° is determined by molecular modeling, and the value of A_1° is determined using the SHIFT ANALYSIS program. Since the structure is not yet refined, it is important to note that only the product of A_jG_i must be known precisely in order to give a reliable set of F_i values. Thus, the analysis is carried out using as a first approximation for G_1° that value obtained from the first energy minimization and then varying A_1° to obtain a minimum value of R. The same value of R and set of F_i° values are obtained by choosing an approximate value of A_1° and varying G_1°. The relatively small values of R ($R = 5.8 \times 10^{-4}$ and 6.9×10^{-4} for the larger ions (Pr^{3+}, Nd^{3+}, Sm^{3+}, and Eu^{3+}) and the smaller ions (Tb^{3+}, Dy^{3+}, Ho^{3+}, Tm^{3+}, Er^{3+}, and Yb^{3+}), respectively) suggest that the F_i values and contact shifts obtained by this method are reliable and were used in the subsequent analyses of the LIS data. The values of the contact shifts are reported in Table 1. Note that, on refining the molecular structure using the SHIFT ANALYSIS program (*vide infra*), good agreement is observed between both the sets of G_i° values (Table 4) and $A_j^\circ = \chi_{zz} - \frac{1}{3}\text{Tr}\chi$ values (Table 5) obtained by the two independent methods of analysis, i.e., least-

squares analysis of the data (eqs 19–22) and those obtained from the SHIFT ANALYSIS program. The self-consistency of the results provides support for the efficacy of this method of computing contact shifts. The values of F_i obtained using eqs 19–22 may be compared with those obtained by the Reilley procedure[30] in Table 4.

In principle, ^{13}C LIS values can be included with ^{1}H data when computing the contact shifts using eqs 19–22. However, the fit of the LIS data was slightly poorer when ^{13}C data were included in the computation of the contact shifts for the larger metal ions (recall that reliable ^{13}C data could not be obtained for the smaller ions). The contact shifts for ^{13}C were thus determined (Table 2) as fitting parameters (eq 5), incorporating the ^{13}C LIS values in the SHIFT ANALYSIS program with the proton data for H_1-H_{10}. However, any nucleus assigned a contact shift as a fitting parameter will show an exact fit between the observed and calculated LIS values for that nucleus. Thus, the ^{13}C contact shifts obtained as fitting parameters are meaningful only if the elements of the susceptibility tensor have been accurately determined from the proton data. The plots of the ^{13}C contact shifts versus $\langle S_z \rangle$, shown in Figure 6, are relatively linear (eq 2) suggesting that the contact shifts obtained by this method are reliable and that the corresponding ^{13}C pseudocontact shifts are consistent with the structural data obtained by analyzing the ^{1}H LIS values.

Refinement of the Structure. Although the MM2 force field does not include parameters involving lanthanide ions, the CAChe molecular modeling program, which uses the MM2 force field, is augmented to include parameters for the lanthanide ions. However, as was noted in the Introduction, the coordination numbers and geometry, as well as the lanthanide donor-atom bond distances, are dictated by the steric requirements of the ligands. Thus, it is unlikely, for any force field, that a set of parameters involving lanthanide ions will provide a reliable minimization for all complexes. However, the CAChe program readily allows changing any of the parameters included within the program. Our approach, then, is to use the analysis of the
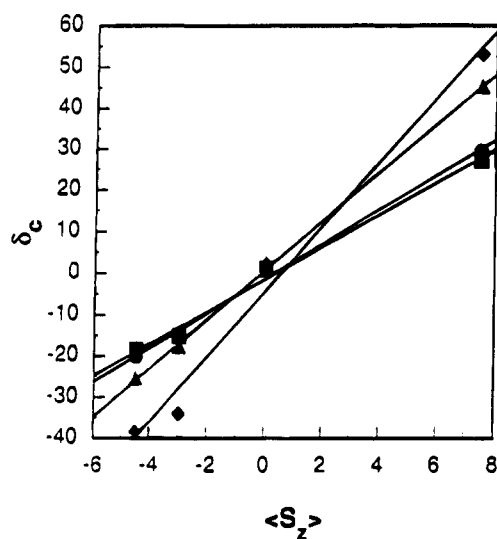
Figure 6. Plots of ^{13}C contact shifts versus $\langle S_z \rangle$ for Ln = Pr, Nd, Eu, and Sm. ■ = C_1, ● = C_2, ▲ = C_3, ● = C_4.

LIS data to establish the idealized Ln−O and Ln−N bond distance parameters to be used in the molecular mechanics calculations. Thus, following separation of the contact shifts, molecular mechanics calculations were carried out using a range of metal−donor atom bond distances (these were the only parameters varied in the augmented MM2 program provided by CAChe). Energy minimization was carried out with the metal−donor atom bond distances locked to the present values, allowing the rest of the molecule to relax. After each minimization, the resulting coordinates of H_1−H_6 were entered into the SHIFT ANALYSIS program, and the goodness of fit of the calculated and observed LIS values as measured by R^2 was determined. Plots of R^2 vs Ln−N and Ln−O bond distances reveal minima corresponding to the bond distances that best fit the LIS data (representative plots for the ytterbium complex are shown in Figure 7). A summary of the metal−donor atom bond distances that produced minima in the plots for each of the complexes and the corresponding values of R are given in Table 6. Althouh not monotonic, a general decrease in M−L donor bond distance is noted across the lanthanide series. Furthermore, the decrease corresponds roughly to that expected due to the decrease in ionic radius across the series for eight-coordinate lanthanide ions:[37] Nd^{3+}−N = 2.82 Å, Yb^{3+}−N = 2.56 Å (9.2% decrease), Nd^{3+}−O = 2.47 Å, Yb^{3+}−O = 2.21 Å (10.5% decrease) vs an 11.2% decrease in ionic radius. With decreasing radius, the metal ion sinks further into the cavity of the macrocyclic ring, allowing the pendant arms to further encapsulate the ion. The result is a decrease in the distance of the metal ion to the mean plane of the nitrogen atoms, with a concomitant increase in the N−Ln−N bond angles, while the distance to the mean plane of the oxygen atoms increases, producing smaller O−Ln−O angles (Table 6). Since the donor atoms were locked in place during minimization, it was also necessary to vary the Ln−N−C(3)−C(4) dihedral angle, which affects rotation of the square pyramid containing the oxygen atoms relative to the square pyramid containing the nitrogen atoms about their common vertex (the Ln^{3+} ion). In the optimal structures, this angle is 32 ± 1° for each complex, producing a rotational angle of 47° (versus 45° in the square antiprism).

As noted above, the pendant arms may be rotated clockwise or counterclockwise, as viewed down the C_4 symmetry axis from the plane of oxygen atoms. Three dihedral angles are required to define the position of the two sets of methylene
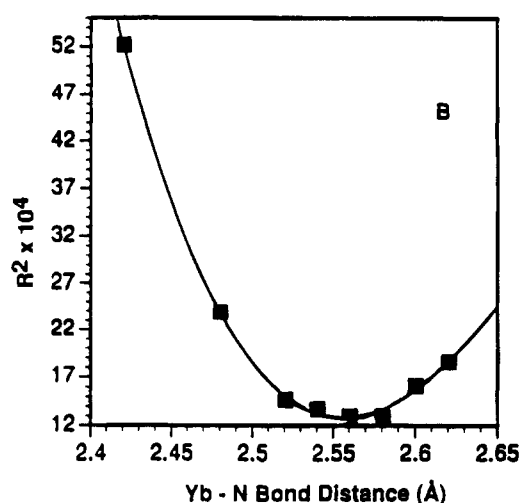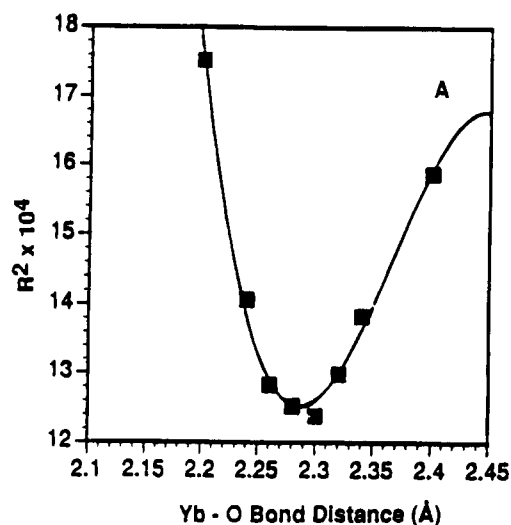
(37) Shannon, R. D. *Acta Crystallogr.* **1976**, *A32*, 751.

Figure 7. Plots of R^2 versus Ln−donor atom bond distances for the ytterbium complex.

Table 6. Lanthanide−Donor Atom Bond Distances (Å) and Bond Angles (deg)

Ln	Ln−N	Ln−O	N−Ln−N	O−Ln−O	Ln−N (plane) (Å)	Ln−O (plane) (Å)	R^a
Pr	2.82	2.47	102	153	1.74	0.63	0.033
Nd	2.82	2.47	102	153	1.74	0.63	0.078
Sm	2.78	2.41	103	150	1.73	0.64	0.026
Eu	2.74	2.30	104	147	1.69	0.68	0.053
Tb	2.64	2.30	109	145	1.54	0.70	0.030
Dy	2.60	2.28	110	142	1.49	0.75	0.035
Ho	2.62	2.30	109	143	1.46	0.78	0.050
Er	2.64	2.33	109	145	1.46	0.79	0.027
Tm	2.54	2.26	112	137	1.41	0.83	0.042
Yb	2.56	2.21	111	138	1.45	0.79	0.034

^{a} Obtained using LIS data for H_1−H_6.

hydrogen atoms (H_6−H_{10}) of the ethyl groups on the pendant arms: $A = \angle C(5)NC(4)C(3)$, $B = \angle C(7)C(6)NC(4)$, and $C = \angle C(8)C(5)NC(4)$. The results reported in Table 1, corresponding to the optimal structures, were obtained using a clockwise rotation of the pendant arms (λ conformation for each of the ethylenediamine rings in the macrocycle) with $A = -141°$, $B = 74°$, and $C = 95°$ for Ln = Pr, Nd, Sm, and Eu and $A = -147°$, $B = 79°$, $C = 62°$ for Ln = Tb, Dy, Ho, Er, Tm, and Yb. Analysis of the LIS data was also carried out with the pendant arms rotated counterclockwise about the C_4 axis, keeping the ethylenediamine rings in the λ conformation (a

diastereomer of the structure described above). Although the Ln—N and Ln—O bond distances in the optimized structures were the same as those obtained in the corresponding complexes with clockwise rotation of the arms, the value of the rotational angle between the two square pyramids was determined to be 28° vs 47° with clockwise rotation of the arms. In each case, the agreement factors were consistently larger for the structures with counterclockwise rotation of the pendant arms. The results of the analysis for the ytterbium complex are presented in Table 1. Although a comparison of the R values for the ytterbium complex (0.10 for counterclockwise rotation vs 0.047 for clockwise rotation) suggests that the clockwise rotation of the arms provides the better fit of the data, it is important to determine at what confidence level the two models are being distinguished on the basis of their respective agreement factors. Richardson et al.[38] reports a statistical method based on the jackknife test that establishes whether two structural models are significantly different on the basis of R values. Applying Richardson's procedure to our data for the ytterbium complex revealed that a model with counterclockwise rotation of the pendant arms can be rejected at the 93% confidence level relative to a model with clockwise rotation of the arms. Similar results were obtained for the other complexes. It should also be noted that the larger value of R obtained for the counterclockwise rotation of the pendant arms is due primarily to disagreement between the observed and calculated LIS values for H_7—H_{10}, i.e., the methylene protons of the pendant arms.][38]

Our results are consistent with those of Morrow et al., who also reported only a single pair of enantiomers in the NMR spectra of lanthanide complexes derived from DOTA analogues with $CH_2CH_2C(O)NH_2$ pendant arms.[8] The crystal structure of the lanthanum complex revealed that the pendant arms were rotated clockwise about the C_4 symmetry axis, when each ethylenediamine ring of the macrocycle is in the λ conformation. In another study using DOTA analogues with 2-hydroxypropyl groups as pendant arms, Morrow et al. observed that the europium complex crystallized with two diastereomers in the unit cell, differing in rotation of the pendant arms.[9] Interestingly, NMR studies of these complexes in methanol-d_4 revealed the presence of only one diastereomer (single pair of enantiomers) in solution. It was proposed that the isomer with clockwise rotation of the pendant arms was favored on the basis of steric considerations. This conclusion is consistent with our results for complexes derived from 1. It is interesting to note that NMR studies revealed the existence of two isomers for the [Ln(DOTA)]⁻ complexes, differing in rotation of the pendant arms.[6e,10] On the basis of both our observations and those reported by others,[6e,8–10] it is apparent that the steric requirements of the pendant arms in DOTA analogues dictate the stereochemistry observed in this class of lanthanide complexes.

Molecular models of complexes derived from 1 reveal that a potential ninth coordination site exists along the C_4 axis, above the plane of oxygen atoms, which could allow for coordination of a solvent molecule. However, when analyses of the LIS values for H_1—H_6 were carried out on models with a coordinated acetonitrile molecule, larger values of R were obtained, e.g., $R = 0.065$ for the ytterbium complex with a coordinated solvent molecule vs 0.034 for the eight-coordinate species. On the basis of the jackknife test, the model with a coordinated acetonitrile molecule can be rejected above the 90% confidence level.

Conclusions

A new computer program for analyzing LIS data is introduced. The success of this program in assigning LIS values to each of the resonances in the spectra of the paramagnetic complexes is demonstrated using lanthanide complexes derived from 1. We have also introduced a new procedure for separating contact shifts from the LIS values. We have shown that analysis of LIS data can be combined with molecular mechanics calculations to determine the structure of lanthanide complexes in solution.

Appendix

The right-hand side of eq 19 can be regarded as the scalar product of the matrices

$$\mathbf{Q}_i = \begin{pmatrix} G_i \\ F_i \end{pmatrix} \text{ and } \mathbf{P}_j = \begin{pmatrix} A_j \\ \langle S_z \rangle_j \end{pmatrix}$$

giving $\delta_{ij} = \mathbf{P}_j^T \mathbf{Q}_i$. The scalar products, and thus the calculated shifts, are invariant for all i and j values under the common transformation matrix,

$$\mathbf{D} = \begin{pmatrix} a & b \\ c & d \end{pmatrix}$$

where $\mathbf{D}$ is any nonsingular 2×2 matrix. For if $\mathbf{Q}'_i = \mathbf{D}\mathbf{Q}_i$ and $\mathbf{P}'_j = (\mathbf{D}^{-1})^T\mathbf{P}_j$, then $(\mathbf{P}')^T\mathbf{Q}_{i'} = \mathbf{P}_j^T\mathbf{Q}_i = \delta_{ij}$. If all the parameters on the right-hand side of eq 19 are allowed to vary in a least-squares fit, four of them cannot be uniquely determined, corresponding to the four real variable parameters of $\mathbf{D}$. If the $\langle S_z \rangle_j$ are fixed, then the form of $\mathbf{D}$ changes to $\mathbf{D} = \begin{pmatrix} a & 0 \\ c & 1 \end{pmatrix}$ from which,

$$(\mathbf{D}^{-1})^T = \begin{pmatrix} \dfrac{1}{a} & -\dfrac{c}{a} \\ 0 & 1 \end{pmatrix}$$

and eqs 20—22 then result. This method can be generalized for cases of three or more terms on the right-hand side of eq 19.

(38) Richardson, M. F.; Rothstein, S. M.; Li, W.-K. *J. Magn. Reson.* **1979**, *36*, 69.